Digest Journal of Nanomaterials and Biostructures Vol. 18, No. 2, April - June 2023, p. 689 - 702

Simulation study on the single droplet evaporation of N-tetradecane with CeO_2 nanoparticles

D. Q. Mei[a,*], J. W. Qi[a], D. M. Guo[b], Y. W. Yan[a], W. D. Zhao[a]
[a]*School of Automotive and Traffic Engineering, Jiangsu University, Zhenjiang 212013, China*
[b]*School of Science, Shandong Jianzhu University, Jinan 250101, China*

To investigate the influence of CeO_2 nanoparticles on the evaporation characteristics of fuel droplets, numerical simulation for single nano-fuel droplet evaporation was conducted based on ANSYS FLUENT software according to the single droplet evaporation visualization experiment. And the effects of nanoparticles' concentration and size on the temperature and fuel-vapor concentration during the evaporation of were emphatically discussed. The simulation results showed that the temperature field and concentration field were distributed in a gradient. Nano-fuel droplets absorbed heat from the external environment, and the temperature of the nano-fuel droplets kept rising until reaching the evaporation equilibrium temperature. The evaporation equilibrium temperature of nano-fuels droplets was higher than that of N-tetradecane (C14) at the temperature of 573 K. In addition, it increased with the increment of nanoparticle concentration and reduction of the nanoparticle size. In the beginning of the evaporation, the vapor volume fraction of nano-fuel was relatively low and it increased slowly with time. As the evaporation process continued, the evaporation rate of nano-fuel droplets increased. The liquid nano-fuel was constantly evaporating to the fuel vapor, and the vapor volume fraction was increased. The vapor volume fraction was increased during the same evaporation period when elevated nanoparticles concentration and minished nanoparticles size.

(Received January 3, 2023; Accepted May 25, 2023)

Keywords: Nanoparticles, Evaporation, Nano-fuel, Droplets, Numerical simulation

1. Introduction

Improving fuel quality is an important measure to strengthen engine combustion, improve thermal efficiency and reduce pollutant emissions. Due to the good thermal conductivity, high specific surface effect and suspension stability of nanoparticles, the addition of nanoparticles to fuel changes the basic physical and chemical parameters such as thermal conductivity and dynamic viscosity of base liquid fuel, which can significantly improve fuel quality, thereby improving combustion and emission performance, and has a wide application prospect [1-4]. Before the fuel enters the cylinder, it will experience the atomization and evaporation stage. However, due to the nanoparticles change the interaction between the base liquid molecules, the mechanism of

* Corresponding author. meideqing@ujs.edu.cn
https://doi.org/10.15251/DJNB.2023.182.689

interphase heat transfer is more complicated, so the evaporation characteristics of nano-fuel droplets become an important basic research content in the field of combustion [5,6].

The atomization and evaporation stage of fuel directly affects the spatial distribution of fuel components and the quality of the mixture, which further affects the combustion and emission process of fuel. The evaporation characteristics of a single fuel droplet can reflect the evaporation performance of the fuel itself to a certain extent. Therefore, it is necessary to explore the law of evaporation process by constructing a micro-scale nano-fuel single droplet evaporation test to provide basic data reference for the heat and mass transfer process of nano-fuel. Currently, some scholars have carried out experimental research on the evaporation characteristics of nanofluids. Javed et al. [7] investigated the evaporation process of Al-kerosene suspension static single droplets in the medium and high temperature environment of 673 ~ 1 073 K. It was found that the evaporation process can be roughly divided into three stages, and the fuel droplets containing higher mass concentration of nanoparticles show obvious microexplosion while studying the effect of nanoparticle mass concentration on droplet evaporation rate. Yan et al. [8] found that the evaporation rate of droplets would change under the condition of hot plate heating, while the evaporation rate remains constant under the condition of plasma heating. Chen et al. [9] investigated the evaporation characteristics of kerosene droplets at different ambient temperatures, and found that in the forced convection environment, the effect of convection velocity on evaporation rate would become increasingly significant with the increase of Reynolds number and Sherwood number.

Owing to the small size of nanoparticles and the existence of irregular motion in the liquid, the mechanism of the flow and heat transfer process of nanofluids becomes very complicated. Experimental studies generally can only provide macroscopic phenomena, and it is difficult to give deeper details. Therefore, numerical simulation of nanofluids is booming. Computational Fluid Dynamics (CFD) is a powerful tool for microscopic analysis of droplet evaporation, especially in heat and mass transfer analysis and flow field prediction [10]. Zigelman et al. [11] investigated the variation of particle distribution with time under different diffusion velocities of nanoparticles by numerical simulation method. The results indicated that the mass concentration distribution of nanoparticles was determined by the competition between particle transfer (convection and diffusion mass transfer) and particle deposition rate inside the droplet. Chereches et al. [12] assumed FLUENT's single-phase homogeneous model to solve the natural convection problem of ZnO water-based nanofluids. Nasrin et al. [13] found that the simulation results are in good agreement with the test results by using the single-phase method in COMSOL software to simulate the performance of nano-fluid photovoltaic thermal (PV/T) system.

Nowadays, the researches' focal spot was mainly on the evaporation test of nanofluid droplets, while the simulation research on the evaporation characteristics of single droplets of oil-based nanofluids is relatively lacking. In addition, the conclusions about how nanoparticles affect the evaporation characteristics of nano-fuel droplets are not consistent, and the numerical model is not perfect enough. Therefore, based on the single droplet evaporation test of nano-fuel, the effects of mass concentration and particle size of CeO2 nanoparticles on the evaporation characteristics of n-tetradecane (hereinafter referred to as C14) fuel droplets were studied by using the EULER multiphase flow model in the computational fluid dynamics software ANSYS FLUENT.

2. Model establishment

2.1. Physical model

Single-phase model and multi-phase model are mainly used to solve the flow and heat transfer of nanofluids. [14] However, nanofluids are essentially a solid-liquid mixture of base fluid and doped nanoparticles, and there are different temperatures and velocities between particles and base fluid. Therefore, compared with the single-phase model, the multiphase flow calculation method is closer to the real situation of nanofluids.

The multiphase flow model is generally divided into Euler-Lagrange method and Euler-Euler method. Eulerian-Lagrangian method is difficult to simulate the reaction system with small particles and mostly used to calculate the simulation of spray and particle load flow. The Euler-Euler method is to treat the discrete phase in the multiphase flow as a fluid. Each phase of the fluid is a continuous medium in the same space and penetrates each other, and has different velocity, temperature and density. The spatial position of each phase is determined by the phase volume distribution function. This method can greatly reduce the amount of calculation and is widely used in various multiphase flow problems.

The evaporation of nano-fuel droplets belongs to the gas-liquid-solid three-phase flow problem. Therefore, the Euler three-phase flow model is used to solve the problem. The third phase is set as solid nanoparticles. The liquid phase and the solid phase are fused with each other. The gas-liquid-solid three-phase is calculated in the Euler system, which can meet the calculation requirements.

The physical evaporation model of CeO2 nano-fuel droplets is shown in Fig. 1. Assuming that the droplets always maintain a uniform spherical shape during the evaporation process, the initial conditions are set as follows: the initial temperature of the droplets is set to 300 K, the ambient temperature is 573 K, and the initial diameter of the droplets is 1 mm. In order to ensure the accuracy of the flow field calculation, it is very important to select the appropriate computational domain size and boundary conditions. If the computational domain is too small, the simulation results will be inaccurate. However, too large computational domain will lead to greatly extended computing time, and ultimately waste of computing resources. After comparison, the computational domain size is set to 20 mm × 20 mm.

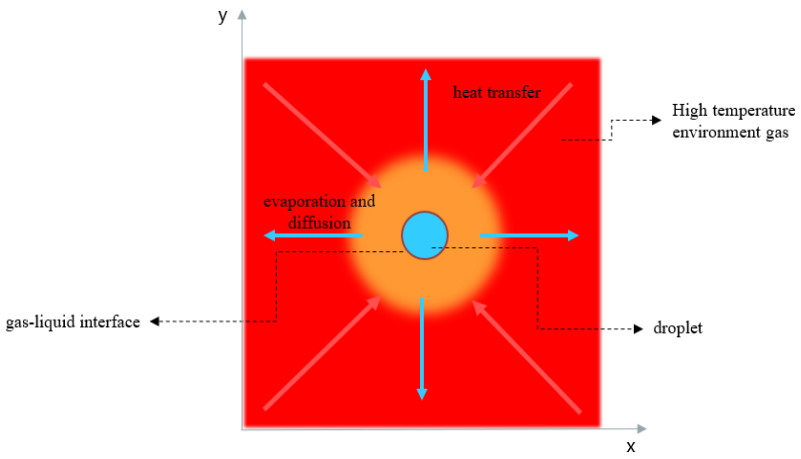

Fig. 1. The physical model of droplet evaporation.

Owing to the evaporation process of nano-fuel droplets involves very complex influencing factors, in order to reduce the difficulty of simulation, it is necessary to simplify and assume the calculation model of nano-fuel droplets. In this model, the temperature difference inside the droplet is ignored, and the temperature distribution inside the droplet is considered to be uniform, and the following assumptions are made [15-17]:

1) Ignore the effect of gravity and assume that droplets remain uniformly spherical during evaporation.

2) Fuel vapor and environmental gas are regarded as rational gas.

3) The dissolution and self-decomposition of droplets in the surrounding gas are not considered.

4) The Soret effect caused by temperature difference and the Dufour effect caused by concentration difference are ignored.

5) Ignore the influence of radiation heat transfer.

2.2. Mathematical model

2.2.1. Euler-Euler multiphase flow model

The evaporation model of the droplets is based on the Lee model in FLUENT, which is a mechanical model based on physical basis, the liquid-gas mass transfer is controlled by the gas phase transport equation. Thus, Equation (1) can be written as:

$$\frac{\partial}{\partial t}(\alpha_{\mathrm{v}}\rho_{\mathrm{v}}) + \nabla \cdot (\alpha_{\mathrm{v}}\rho_{\mathrm{v}}\overline{V_{\mathrm{v}}}) = \dot{m}_{\mathrm{bv}} \tag{1}$$

where v is the gas phase; α_{v} is the gas volume fraction; ρ_{v} is the gas phase density; $\overline{V_{\mathrm{v}}}$ is the gas phase velocity; $\dot{m}_{\mathrm{bv}}$ is the mass transfer rate of evaporation, which specific expression is as follows:

$$\dot{m}_{bv} = \mathrm{coeff}\,\frac{\alpha_{\mathrm{b}}\rho_{\mathrm{b}}(T_{\mathrm{b}} - T_{\mathrm{sat}})}{T_{\mathrm{sat}}} \tag{2}$$

where T_{sat} is saturation temperature; coeff is the factor controlling the phase transition intensity; α_{b}, ρ_{b} and T_{b} are the volume fraction, density, and temperature of the liquid phase, respectively.

2.2.2. Control equations

In the Euler-Euler method, different phases are treated as interpenetrated continuums. Owing to the volume occupied by one phase can no longer be occupied by other phases, the concept of phase volume fraction is introduced. The volume fraction is a continuous function of time and space, and the sum of the volume fractions of each phase is equal to 1.

The calculation formulas of local evaporation flow rate, total evaporation rate and gas-liquid interface heat transfer of nano-fuel droplets are as follows [13]:

$$j_{\mathrm{L}} = \frac{M\left(D\nabla c\right)}{\rho} \tag{3}$$

$$j_V = \int_S j_L dS \tag{4}$$

$$q = -\bar{m} h_t \tag{5}$$

where j_L is the local evaporation flow rate of nano-fuel droplet evaporation; M is the molar mass (mole fraction) of fuel vapor; the vapor concentration; c is the vapor diffusion coefficient in the gas phase region; D is the density of fuel vapor; ρ is the evaporation rate of nano-fuel droplet evaporation; j_v is the volume of nano-fuel droplet evaporation per unit time; S is the cross-sectional area of fuel vapor; q is the heat transfer at the gas-liquid interface per unit time; $\bar{m}$ is the mass flow rate of vapor when the droplet evaporates; h_t is the latent heat for vaporization.

3. Model validation

3.1. Mesh independence verification

The computational accuracy of the simulation depends largely on mesh division Reasonable mesh division method can effectively reduce calculation amount while ensuring calculation accuracy [18]. Therefore, it is necessary to verify the mesh independence to determine the most suitable size conditions.

The C14 droplet was used as the experimental object. The ambient temperature was 573 K, the initial droplet temperature was 300 K, and the droplet diameter was 1 mm. As shown in Table 1, four different mesh division schemes were set up in the simulation, in which the number of meshes occupied by droplets was 69, 316, 7 860 and 31 401, respectively, and the surface area of droplets was also slightly different. According to the time step of 1e-6, the maximum number of iterations per step was 30, and the same number of iterations was used. The change of temperature in the computational domain was used as the index of mesh independence test, while the test scheme 4 with the largest number of meshes was used as the reference group. The calculation results errors between schemes 1-3 and scheme 4 are calculated respectively.

Table. 1. Mesh independence design and comparison of simulation results.

Schemes	Mesh number	Mesh size / (mm×mm)	Droplet surface area / mm^2
1	38 416	0.05×0.05	0.69
2	160 000	0.01×0.01	0.79
3	4 000 000	0.005×0.005	0.786
4	10 000 960	0.001×0.001	0.785

The accuracy of calculation results is greatly affected by the size of the mesh, Mesh independence verification for four different design scenarios were shown in Figure 2. It can be seen from the figure that the calculation results of scheme 1 and scheme 4 have the largest

difference. However, the calculation results of scheme 3 and scheme 4 are convergent. The results show that as the mesh size decreases, its influence on the calculation results decreases rapidly, though the effect of mesh size on computational accuracy is negligible when mesh number increases to a certain extent. Although the more the number of meshes, the more accurate the calculation results, however, too small mesh size will make the calculation time multiply. Forasmuch as mesh size of scheme 4 is relatively small, the calculation time of scheme 4 is greatly prolonged compared with scheme 3. Considering the relatively simple geometric structure of the model, combined with the economy and accuracy of the calculation, after considering all factors, the mesh size of scheme 3 is selected for the next simulation study.

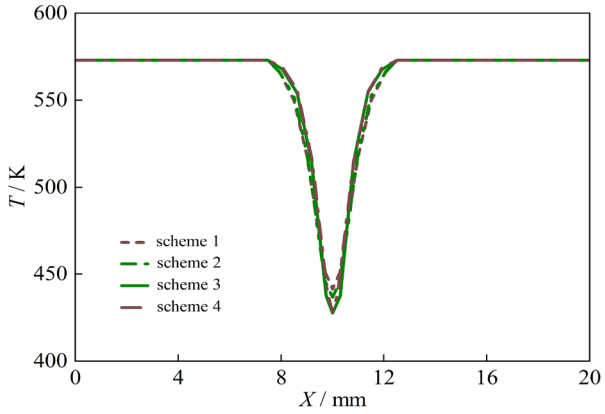

Fig. 2. Verification of mesh independence.

3.2. Single droplet evaporation test model validation

In order to verify the accuracy of the evaporation model, the nano-fuel with C14 as the base fuel and CeO2 with particle sizes of 20 nm and 50 nm as nanoparticles was selected to carry out the single droplet evaporation test of nano-fuel. Based on the two-step method [19], 50 mg / L, 100 mg / L and 150 mg / L nano-fuel oil samples were prepared respectively. For the convenience of expression, the mass concentration and particle size of the particles are represented by the above and the subscripts respectively. For example, Ce_{20}^{50} represents CeO2 nano-fuel with a mass concentration of 50 mg / L and a particle size of 20 nm.

Figure 3 shows a schematic of the experimental setup used to analyze the evaporation of nano-fuel single droplets, which consists of an evaporation cylinder, temperature controller, hanging drop, screw, computer and high-speed camera. The temperature control device is mainly composed of a resistance wire and a thermocouple, which is heated by a resistance wire to increase the temperature in the cylinder to meet the test conditions. The droplet conveying device is mainly composed of a ball screw, a quartz wire and a stepping motor. The high-speed camera is in the opposite direction of the illumination set to enhance the contrast and visualize the droplet evaporation process. The illumination set comprises a LED light and a diffusion glass. The two quartz wires are fixed at the bottom end of the ball screw in a cross shape, and the center intersection part is used for carrying and suspending droplets. The volume of a single suspended droplet is about 0.5 μL, which is produced by a micro sampler. The morphology change of Ce_{20}^{50} nano-fuel droplet during evaporation at 573 K is shown in Fig. 4.

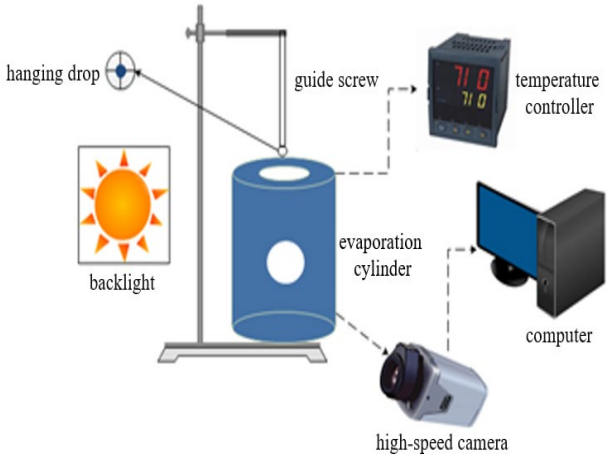

Fig. 3. Schematic diagram of single droplet evaporation device.

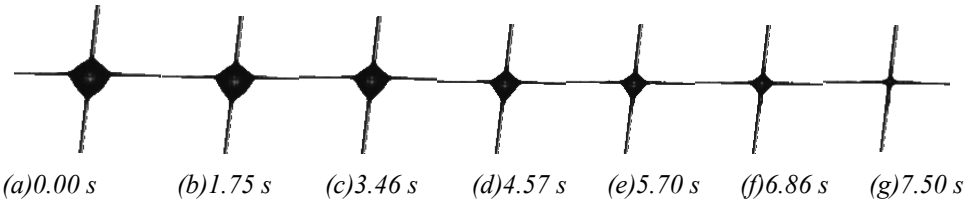

Fig. 4. Morphology change of Ce_{20}^{50} nano-fuel droplet during evaporation at 573 K.

On the basis of the mesh size determined above, the numerical simulation of the evaporation process of Ce_{20}^{50} nano-fuel droplets is carried out, and the simulated droplet diameter changing with time is compared with the experimental data, as shown in Fig. 5. The initial conditions of Ce_{20}^{50} nano-fuel droplets are set as follows: the initial temperature of droplets is 300 K, the ambient temperature is 573 K, and the initial diameter of droplets is 1 mm. It can be seen from the figure that there are some differences between the simulation results and the experimental results in the set time range, which is reflected in the fact that the change of the droplet diameter of the simulation results is always faster than the experimental value. The reason for this phenomenon is that the error is difficult to completely eliminate during the test, and there is a certain degree of heat loss, which cannot be used for evaporation. Owing to the good consistency of trends between the numerical analysis results and the experimentation results, the established model is proved to be reasonable.

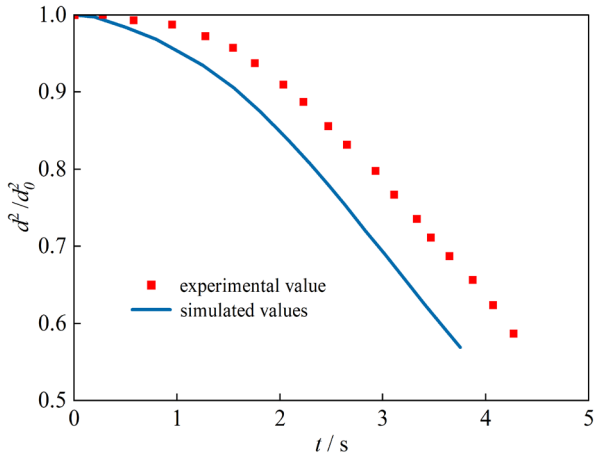

Fig. 5. Comparison of measured droplet diamerters with simulated results varying with time during the evaporation of Ce_{20}^{50} *nano-fuel.*

4. Simulation results and analysis

4.1. Temperature change of droplet evaporation process

The heat transfer ability of liquid phase can be reflected by the change of droplet temperature field to some extent. At the ambient temperature of 573 K, the temperature field change of Ce_{20}^{50} nano-fuel droplet evaporation process, as shown in figure 6. The temperature difference exists between the high temperature environment and the Ce_{20}^{50} nano-fuel droplets, and the nano-fuel droplets and the high temperature environment exchange heat through natural convection and heat conduction. In convective heat transfer, when the fluid flows through the fluid or solid surface with different temperatures, the temperature of the fluid in the normal direction of the contact surface between the two will change significantly due to different temperatures, resulting in a temperature gradient.

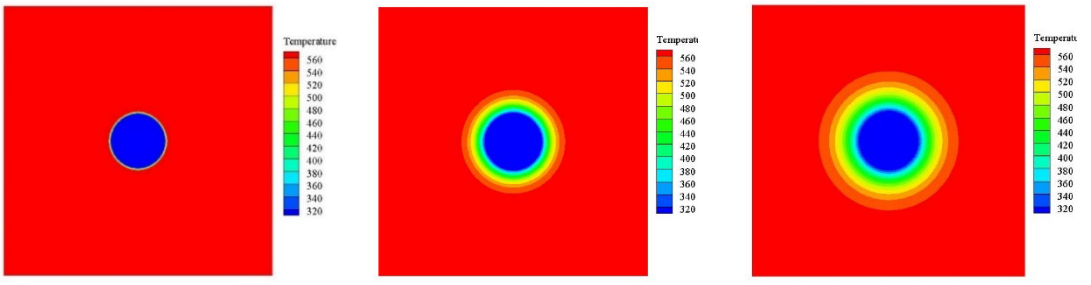

(a) t=0.0 s *(b) t=0.1 s* *(c) t=0.2 s*

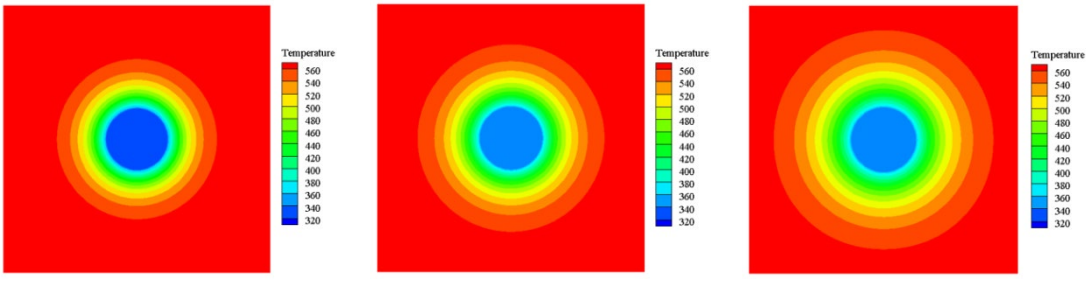

(d) t=0.3 s *(e) t=0.4 s* *(f) t=0.5 s*

Fig. 6. Temperature field of Ce_{20}^{50} *nano-fuel droplet during evaporation at 573 K.*

The evaporation equilibrium temperature is used to measure the change of droplet temperature [20]. When evaporating in a high temperature environment, driven by the temperature difference, the heat is continuously transferred from the high temperature environment to the low temperature droplet, part of which is used to make the droplet temperature rise rapidly, and the other part is provided to the liquid molecule as the heat consumed during evaporation. Therefore, the droplet temperature does not rise to the same temperature as the external environment, but gradually rises to a certain temperature and then remains basically unchanged, that is, the evaporation equilibrium temperature of the droplet, and the stage of droplet endothermic heating is the instantaneous heating stage.

At 573 K, the evaporation equilibrium temperature of $^{Ce_{20}}$ nano-fuel droplets with different mass concentrations is shown in figure 7. The evaporation equilibrium temperatures of nano-fuel droplets increase with the increase of nanoparticle mass concentration at 573 K, which are 469.8 K, 472.8 K and 474.6 K, respectively. Compared with C14, they are increased by 1.5 %, 2.3 % and 2.7 %, respectively. Fig. 8 presents the instantaneous heating stage of nano-fuel droplets with different mass concentrations at 573 K. The instantaneous heating stage of nano-fuel droplets lasts 1.58 s. 22.9 % of the total duration of evaporation; the instantaneous heating stage of nano-fuel droplets is 1.41 s, accounting for 21.4 % of the total evaporation time. With the increase of particle mass concentration, the instantaneous heating stage of nano-fuel droplets accounts for a smaller proportion of the total evaporation stage, which is conducive to promoting evaporation. This is because the addition of nanoparticles greatly increases the thermal conductivity of the base fuel, and can absorb more heat from the outside at the same time. At the same time, the specific heat capacity of nanoparticles, as a solid, is relatively small compared with that of the base liquid, and its temperature rises faster than that of the base liquid, which will also increase the equilibrium temperature of the droplets to a certain extent. Therefore, the higher the particle mass concentration is, the higher the evaporation equilibrium temperature of nano-fuel droplets is; at the same time, the shorter the transient phase of the droplet, the faster the droplet can enter the stable evaporation stage, accelerating the evaporation process of the fuel droplet, which is conducive to the evaporation of the droplet.

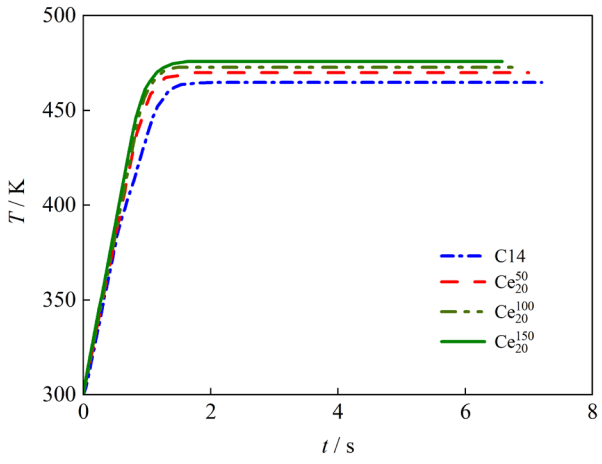

Fig. 7. Evaporation equilibrium temperatures of $^{Ce_{20}}$ nano-fuel droplet.

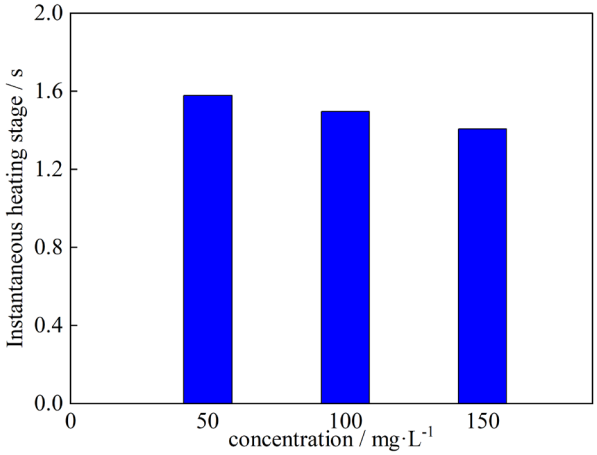

Fig. 8. Instantaneous heating stage of $^{Ce_{20}}$ *nano-fuel droplet with various mass concentrations.*

The evaporation equilibrium temperature varies with the particle size of the nanoparticles in the base fuel. At 573 K temperature conditions, the evaporation equilibrium temperature of different particle sizes Ce_{20}^{50} and Ce_{50}^{50} nano-fuel droplets is shown in figure 9. The evaporation equilibrium temperature of Ce_{20}^{50} nano-fuel droplets is 469.8 K, while that of Ce_{50}^{50} nano-fuel droplets is 467.3 K. It can be seen that the evaporation equilibrium temperature of fuel droplets containing large-size nanoparticles is lower. Fig. 10 presents the instantaneous heating stage of different particle sizes Ce_{20}^{50} and Ce_{50}^{50} nano-fuel droplets. It can be seen from Fig. 10 that the instantaneous heating time of Ce_{20}^{50} and Ce_{50}^{50} nano-fuel droplets is 1.58 s and 1.61 s, respectively, accounting for 22.9 % and 23.1 % of the total evaporation time of and nano-fuel droplets, respectively. This is due to the fact that at the same mass fraction, the number of large particle size particles is relatively small, and the heat transfer interface between particles and liquid is relatively small, and the heat transfer ability is relatively weak, resulting in a relatively slow heating rate of droplets and a relatively low evaporation equilibrium temperature of droplets.

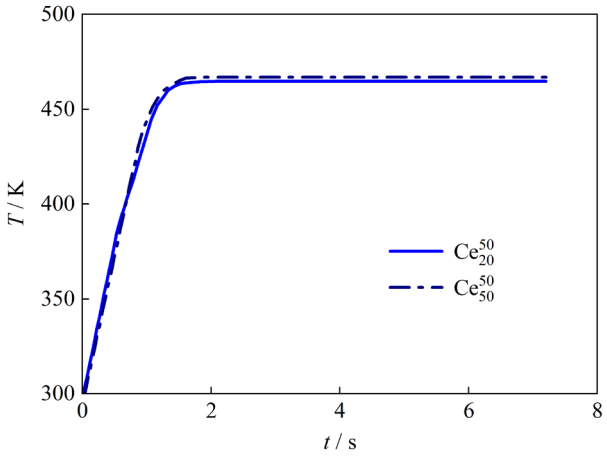

Fig. 9. Evaporation equilibrium temperatures of $^{Ce_{20}^{50}}$ *and* $^{Ce_{50}^{50}}$ *nano-fuels droplet.*

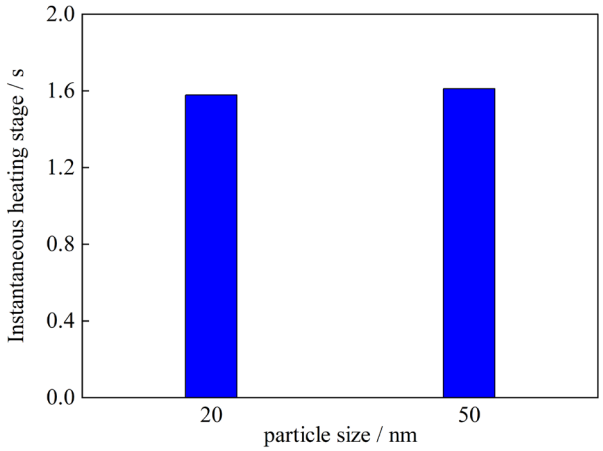

Fig. 10. Instantaneous heating stage of Ce_{20}^{50} *and* Ce_{50}^{50} *nano-fuels droplets.*

4.2. Change of mass concentration in droplet evaporation process

Fig. 11 presents the change of mass concentration field in the evaporation process of Ce_{20}^{50} nano-fuel droplets at 573 K ambient temperature. Learned from Fig. 11, as the evaporation process continues to advance, the fuel vapor gradually accumulates on the surface of the droplet, and continues to diffuse to the surrounding environment driven by a huge mass concentration difference, resulting in convective conduction of the fuel vapor. The diffused fuel vapor is axisymmetrically distributed in the computational domain, and the concentration gradually decreases outward along the droplet center to generate a mass concentration gradient. Similar to the temperature boundary layer, when there is a concentration difference between the fluid and the phase interface, it is under the combined action of molecular diffusion and convective mass transfer. The droplet will undergo mass transfer during the evaporation process. As the evaporation process continues, the volume fraction of the liquid phase is also decreasing.

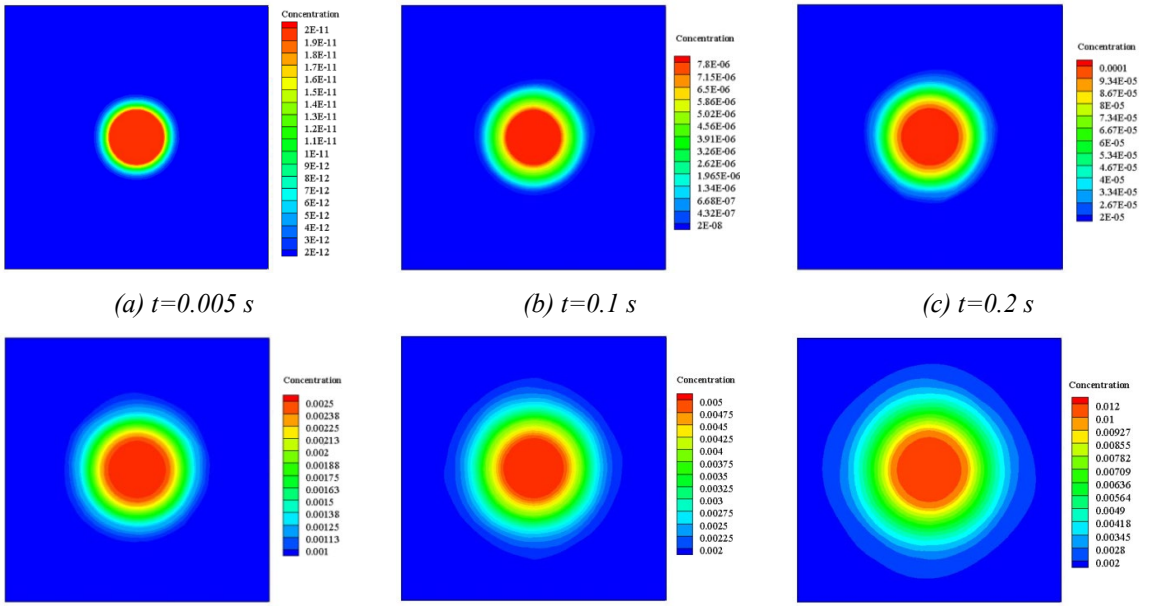

(a) t=0.005 s *(b) t=0.1 s* *(c) t=0.2 s*

(d) t=0.3 s *(e) t=0.4 s* *(f) t=0.5 s*

Fig. 11. Mass concentration field of Ce_{20}^{50} *nano-fuel droplet during evaporation.*

The change of fuel vapor volume fraction during the evaporation of Ce_{20} nano-fuel droplets with different mass concentrations is shown in Fig.12. Learned from Fig. 12, at the starting point of evaporation, the volume fraction of gas phase is 0. As the evaporation process progresses, the fuel vapor gradually accumulates and the volume fraction of fuel vapor gradually increases. The change of the volume fraction of fuel vapor with time can be roughly divided into two stages: in the initial stage, the change rate of the volume fraction of gas phase with time is small, and then the volume fraction of gas phase increases rapidly with time. It is convenient to describe below. The time point divided into two stages is defined as tθ. There are differences in the change of gas phase volume fraction of nano-fuel with different mass concentrations. Among them, the change rate of gas phase volume fraction of Ce_{20}^{150} nano-fuel droplets with time is the fastest, and the change rate of gas phase volume fraction of Ce_{20}^{50} nano-fuel droplets with time is relatively slow. The time defining points of dividing Ce_{20}^{50} and Ce_{20}^{150} nano-fuel into two stages are tθ1 and tθ2 respectively., respectively. At the time of tθ, the gas phase volume fraction of Ce_{20}^{50} nano-fuel droplets is 0.116, and the gas phase volume fraction of Ce_{20}^{150} nano-fuel droplets is 0.121, which is increased by 4.3 %. The higher the mass concentration of nanoparticles, the more favorable it is to promote the conversion of liquid phase to gas phase. This is due to the higher the mass concentration of nanoparticles contained in the base liquid, the higher the evaporation equilibrium temperature of the droplets, the more energy the liquid phase molecules obtain, and the faster the gas-liquid phase transition rate.

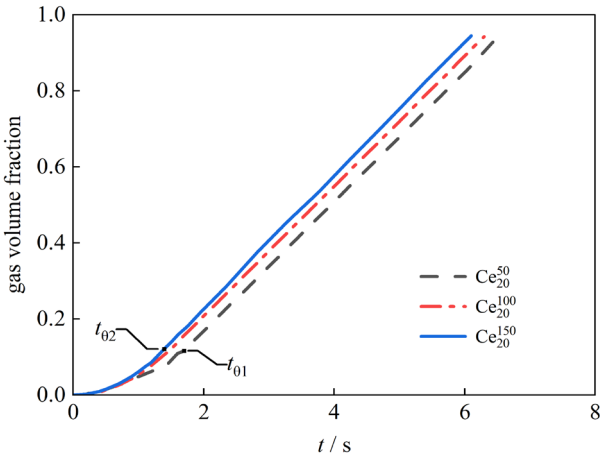

Fig. 12. Vapor volume fraction of Ce_{20} nano-fuel droplet evaporation with different concentrations.

In the evaporation process of nano-fuel droplets, the change of volume fraction of fuel vapor with different particle sizes is shown in Fig.13.The figure shows that the particle size of nanoparticles also affects the change rate of gas phase volume fraction of fuel vapor. The change rate of the gas phase volume fraction of Ce_{20}^{50} nano-fuel droplets is faster than that of Ce_{50}^{50} nano-fuel droplets. The time defining points of dividing Ce_{20}^{50} and Ce_{50}^{50} nano-fuel into two stages are tθ3 and tθ4, respectively. At the time of tθ, the gas phase volume fraction of Ce_{50}^{50} nano-fuel droplets is 0.104, which is 10.3 % lower than that of Ce_{20}^{50} nano-fuel droplets. This is due to the slow heat transfer efficiency between large-sized nanoparticles and base liquid. The ability to

increase the internal temperature of the droplet is relatively weak, so the effect of promoting droplet evaporation is relatively weak for nanoparticles with relatively small particle size, and the rate of evaporation of liquid molecules into fuel vapor is relatively slow.

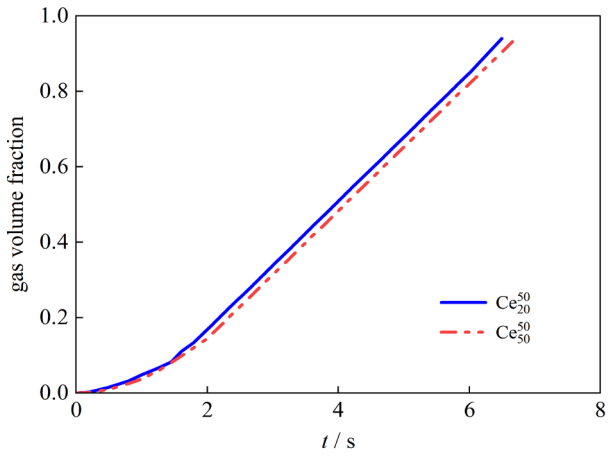

Fig. 13. Vapor volume fraction of nano-fuel droplet evaporation with different particle sizes.

5. Conclusion

1) The single droplet evaporation model of nano-fuel was constructed on the basis of the EULER multiphase flow model, droplet evaporation test data was taken as the reference at the same time, and its calculation accuracy was verified to meet the requirements. Furthermore, the effects of CeO2 nanoparticle mass concentration and particle size on the evaporation characteristics of fuel droplets were analyzed.

2) In the early stage of evaporation, owing to the low temperature of droplets, the rate of liquid phase to gas phase conversion is slow, and the gas phase volume fraction is relatively small. However, as the heat is continuously transferred between the gas and liquid, the temperature of the nano-fuel droplets gradually increases, and sufficient energy is given to the liquid molecules, which continuously evaporates into fuel vapor, and the gas phase volume fraction increases rapidly with time. The volume fraction of gas phase of droplets tended to rise up with increasing the nanoparticles mass concentration or diminishing nanoparticles size, and the more conducive to promoting liquid phase gasification during the same evaporation period.

3) At the ambient temperature of 573 K, the evaporation equilibrium temperature of each nano-fuel is higher than that of C14. The evaporation equilibrium temperature of droplets tended to rise up with increasing the nanoparticles mass concentration or diminishing nanoparticles size, and the greater the energy obtained by the liquid molecules, the more conducive to promoting evaporation.

Acknowledgments

The authors sincerely appreciate the support provided by China Scholar Council and the National Natural Science Foundation of China (No. 51876082).

References

[1] Chen A F, Adzmi M A, Adam A, et al., Energy Conversion and Management, 2018, 171: 461-477; https://doi.org/10.1016/j.enconman.2018.06.004
[2] Jiang L, Xie X L, Wang L W, et al., Applied Thermal Engineering, 2018, 134: 29-38; https://doi.org/10.1016/j.applthermaleng.2018.01.116
[3] Fayyazbakhsh A, Pirouzfar V., Fuel, 2016, 171: 167-177; https://doi.org/10.1016/j.fuel.2015.12.028
[4] Tiwari H P, Banerjee P K, Saxena V K., Fuel, 2013, 107: 615-622; https://doi.org/10.1016/j.fuel.2012.12.015
[5] Bakthavatchalam B, Habib K, Saidur R, et al., Journal of Molecular Liquids, 2020, 305: 112787; https://doi.org/10.1016/j.molliq.2020.112787
[6] Yan X, Xu J L, Meng Z J, et al., Applied Thermal Engineering, 2020, 175: 115389; https://doi.org/10.1016/j.applthermaleng.2020.115389
[7] Javed I, Baek S W, Waheed K., Experimental Thermal and Fluid Science, 2014, 56: 33-44; https://doi.org/10.1016/j.expthermflusci.2013.11.006
[8] Yan X, Xu J, Meng Z, et al., Applied Thermal Engineering, 2020, 175, 115389; https://doi.org/10.1016/j.applthermaleng.2020.115389
[9] Chen L F, Li G Z, Fang B., International Journal of Multiphase Flow, 2019, 114: 229-239; https://doi.org/10.1016/j.ijmultiphaseflow.2019.03.012
[10] Behroyan I, Vanaki S M, Ganesan P, et al., International Communications in Heat and Mass Transfer, 2016, 70: 27-37; https://doi.org/10.1016/j.icheatmasstransfer.2015.11.001
[11] Zigelman A, Manor O., Journal of Colloid and Interface Science, 2018, 509: 195-208; https://doi.org/10.1016/j.jcis.2017.08.088
[12] Nasrin R, Rahim N A, Fayaz H, et al., Renewable Energy, 2018: S0960148118300144; https://doi.org/10.1016/j.renene.2018.01.014
[13] Omid M, Lioua K, Mohammad A. et al., Physics Reports, 2019, 791: 1-59; https://doi.org/10.1016/j.physrep.2018.11.003
[14] Behroyan I, Vanaki S M, Ganesan P, et al., International Communications in Heat and Mass Transfer, 2016, 70: 537-558; https://doi.org/10.1016/j.icheatmasstransfer.2015.11.001
[15] Pinheiro A P, Vedovoto J M., Flow, Turbulence and Combustion, 2019, 102(3): 537-558; https://doi.org/10.1007/s10494-018-9973-8
[16] Zhang L, Kong S C., Chemical Engineering Science, 2009, 64(16): 3688-3696; https://doi.org/10.1016/j.ces.2009.05.013
[17] Tamim J, Hallett W L H., Chemical Engineering Science, 1995, 50(18): 2933-2942; https://doi.org/10.1016/0009-2509(95)00131-N
[18] Sheng Y, Wang M Y, Zhang L, et al., Powder Technology, 2022, 396: 785-793; https://doi.org/10.1016/j.powtec.2021.11.034
[19] Bakhtiari R, Kamkari B, Afrand M, et al., Powder Technology, 2021, 385: 466-477; https://doi.org/10.1016/j.powtec.2021.03.010
[20] Wu M R, Wang M, Zhang Y Y, et al., Enzyme and Microbial Technology, 2020, 142: 109690; https://doi.org/10.1016/j.enzmictec.2020.109690